Responses to reviewer 2#'s comments point by point

MS No.: essd-2022-436

Title: A grid dataset of leaf age-dependent LAI seasonality product (Lad-LAI) over tropical and subtropical evergreen broadleaved forests

Author(s): Xueqin Yang et al.

General Comments of Reviewer 2#:

This work produced the first grid dataset of leaf age-dependent LAI product that is classified into young, mature, and old types, over the tropical evergreen broadleaved forests from satellite observations. It is an interesting work, and the overall framework is clear. The topic fits the ESSD, but there are still some major issues in this work that need to be addressed before this manuscript can be published. Some overall and point-to-point are provided below. I hope these comments are useful and constructive to improve this manuscript.

Response: *Thanks for the valuable comments and nice suggestions. We have carefully studied them and made corresponding revisions in the revised manuscript. The point-to-point responses are listed below.*

Major Comments:

Comment 1: The manuscript need to be thoroughly polished.

Response: *Thanks. We have thoroughly revised the manuscript following the reviewer's comments, e.g. totally rewrote the Introduction (see responses to Comment 4), added Study area and data (see responses to Comment 5), added new sites for validations (see responses to Comment 3), added new analyses of uncertainties (see responses to Reviewer 3#). Finally, we also asked a company to polish our English language, including grammar, syntax, and sentence structure, to improve the readability of the manuscript.*

Comment 2: Abstract cannot summarize this work well, particularly for describing results, accuracy, and performance (Lines 37-48). Alternatively, add some quantitative metrics in Abstract, e.g., how much accuracy can be reached for the site- and continental-scale validation and comparison (Lines 38-43), and how LAI cohort perform well with satellite data analysis (Lines 45-48), and also, using concise language to shorten Lines 49-52.

Response: *Thank your suggestions. To better summarize the results, accuracy, and performance, we have added some quantitative metrics to the abstract. Specifically, we found that our approach achieved accuracy of* $R^2_{young}=0.41$, $R^2_{mature}=0.62$, $R^2_{old}=0.63$ *for* LAI_{young}, LAI_{mature} *and* LAI_{old} *compared to in situ observation. On the regional average, the mean correlation coefficient between monthly EVI and* $LAI_{young+mature}$ *was up to 0.61. Furthermore, the Lad-LAI can capture the spatial pattern of dry-season "green-up" in satellite data analysis. Finally, we streamlined the language in original manuscript lines 49-52. The abstract revised as suggested as follows:*

"Quantification of large-scale leaf age-dependent leaf area index has been lacking in tropical and subtropical evergreen broadleaved forests (TEFs) despite the recognized

*importance of leaf age in influencing leaf photosynthetic capacity in this region. Here, we simplified the canopy leaves of TEFs into three age cohorts, i.e., young, mature and old one, with different photosynthesis capacity ($V_{c,max}$) and proposed a novel neighbor-based approach to develop a first monthly grid dataset with 0.25-degree spatial resolution of leaf age-dependent LAI product (**referred to as Lad-LAI**) during 2001-2018 over the continental scale from satellite observations of sun-induced chlorophyll fluorescence (SIF) that was reconstructed from MODIS and TROPOMI (the TROPOspheric Monitoring Instrument) as a proxy of leaf photosynthesis. The new Lad-LAI products showed good seasonality of three LAI cohorts, i.e., young (LAI_{young}) (R^2=0.41), mature (LAI_{mature}) (R^2=0.62) and old (LAI_{old}) (R^2=0.63) leaves, at the eight sites (four in south American, three in subtropical Asia and one in Congo) and also performed well in representing their interannual dynamics, with R^2 being equal to 0.30, 0.41 and 0.24 for LAI_{young}, LAI_{mature} and LAI_{old} at Barrocolorado site, respectively. Additionally, the days when LAI_{old} decreases sharpest are mostly consistent with those of seasonal litterfall peaks at 53 in situ measurements across the whole tropical region (R=0.82). The LAI seasonality of young and mature leaves also agree well with the Enhanced Vegetation Index (EVI) products (R=0.61), which is a good proxy of effective leaves. The spatial patterns clustered from the three LAI cohorts coincide with those clustered from climatic variables and can also capture a dry-season green-up of canopy leaves across the wet Amazonia areas where mean annual precipitation exceeds 2,000 mm yr^{-1}, consistent with previous satellite data analysis. We added GOSIF-derived GPP and FLUXCOM GPP to test the potential uncertainties caused by GPP estimation based on SIF-GPP relationship. RTSIF-derived GPP based on simple SIF-GPP relationship showed the highest correlation with LAI_{young}, LAI_{mature} and LAI_{old} at 8 observed sites among the three versions. The new Lad-LAI also show stable seasonality in LAI_{young}, LAI_{mature} and LAI_{old} across the whole tropical region based on both 2*2 and 4*4 neighboring pixels, with R being equal to 0.63, 0.68 and 0.95, respectively. Here, we provide the average seasonality of three LAI cohorts as the main dataset, and their time-series as a supplementary dataset. The Lad-LAI products are available at https://doi.org/10.6084/m9.figshare.21700955.v3 (Yang et al., 2022)."*

Comment 3: I just concerned the results were validated by only three sites (one in subtropical Asia and two in Amazon). Can not find more sites to validate? For example, eddy covariance data and may find more details from papers (DOI: 10.1126/science.aad5068; https://doi.org/10.1016/j.agrformet.2013.04.031). More ground validation can show the robustness and accuracy of this dataset.

***Response**: Thanks. The sites of the first literature provided by the reviewer are K67 and K34 sites in original manuscript Figure 5 that have been used for validations in this study. For the second literature provided by the reviewer, there is no observed LAI seasonality with different leaf age cohorts (young, mature and old) although it also applied a simple leaf-flush model to simulate leaves variability.*

Following the reviewer's suggestion, in the new version, we added 5 more sites to validate the LAI datasets, e.g. Barrocolorado site in Panama, eucflux site in southern Amazon, congoflux site in Congo, Gutian and Banna sties in subtropical China.

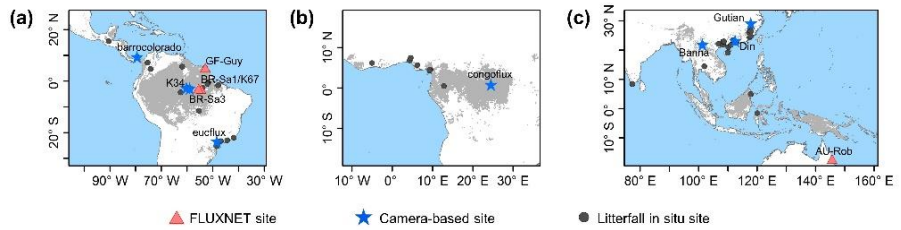

Figure 1. *Study areas over tropical and sub-tropical for evergreen broadleaves forests. Red triangles: four sites of EC-observed GPP seasonality. Blue pentangles: camera-based observation sites of three LAI cohort seasonality. Black circles: observation sites of litterfall seasonality.*

Till now, there are totally 8 sites for ground validations. Validation results were shown in Figures 3-5. All ground observations are consistent with the proposed Lad-LAI products. Please see details in the revised manuscript.

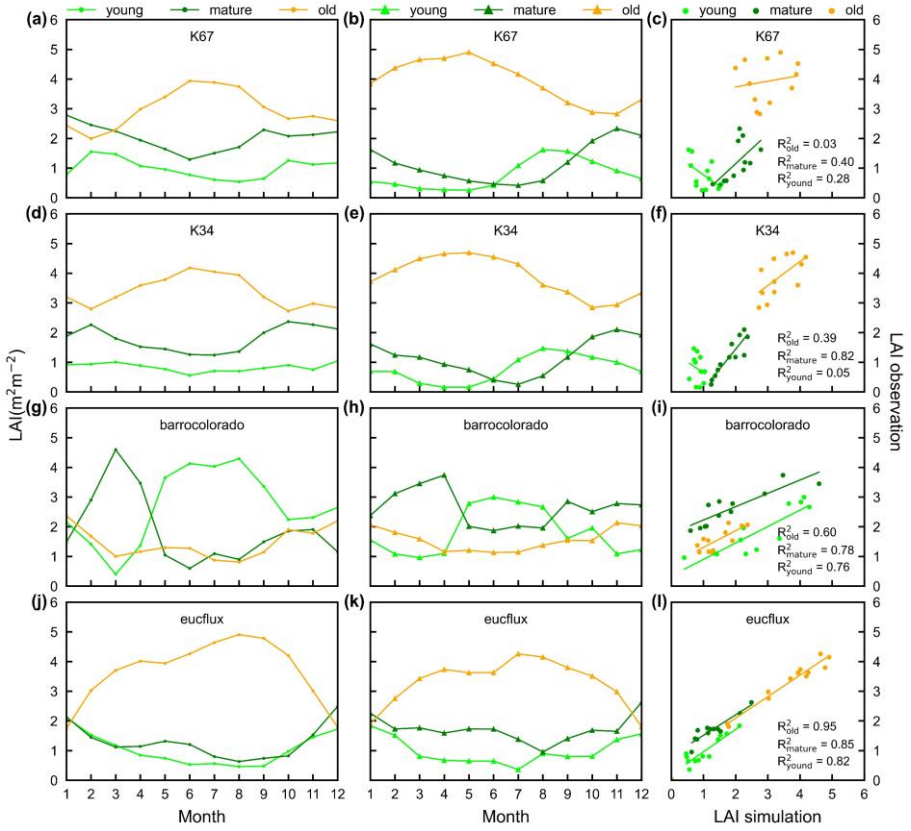

Figure 3. *Seasonality of simulated LAI_{young}, LAI_{mature}, and LAI_{old} in comparison with observed data at 4 sites in South American. (panels a, d, g and j) simulated LAIs; (panels b, e, h and k) observed LAIs; (panels c, f, i and l) scatterplots between simulated and observed LAIs. Limegreen dots are LAI_{young}; green dots are LAI_{mature}; orange dots are LAI_{old}.*

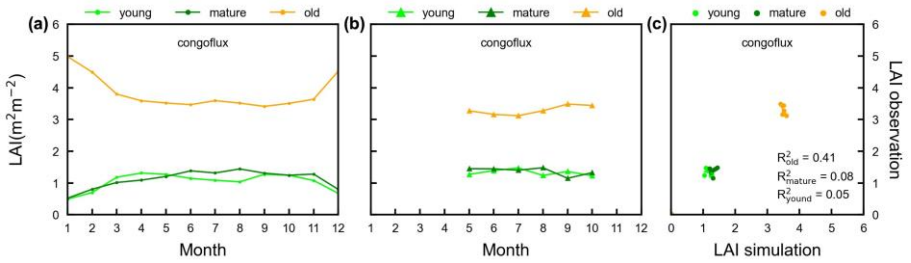

Figure 4. *Seasonality of simulated LAI_{young}, LAI_{mature}, and LAI_{old} in comparison with observed data at one site in Congo. (a) simulated LAIs; (b) observed LAIs; and (c) scatterplots between simulated and observed LAIs. Limegreen dots are LAI_{young}; green dots are LAI_{mature}; orange dots are LAI_{old}.*

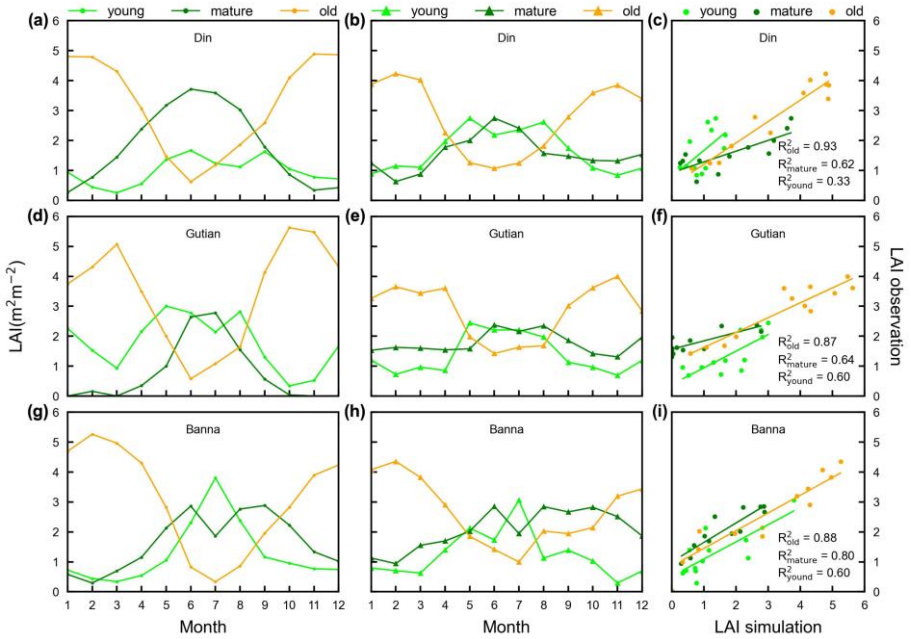

Figure 5. *Seasonality of simulated LAI_{young}, LAI_{mature}, and LAI_{old} in comparison with observed data at 3 sites in tropical Asia. (panels a, d and g) simulated LAIs; (panels b, e and h) observed LAIs; (panels c, f and i) scatterplots between simulated and observed LAIs. Limegreen dots are LAI_{young}; green dots are LAI_{mature}; orange dots are LAI_{old}.*

Comment 4: Introduction can be considered to re-organize, as the current version seems lack some logics and useful information.

Response: *Thanks for the comments on the introduction section. We have reorganized it as follows:*

"Tropical and subtropical evergreen broadleaved forests (TEFs) account for approximately 34% of global terrestrial primary productivity (GPP) (Beer et al., 2010) and 40-50% of the world's gross forest carbon sink (Pan et al., 2011; Saatchi et al., 2011). Despite a perennial canopy, TEFs shed and rejuvenate their leaves continuously throughout the year, leading to significant seasonality in canopy leaf demography (Wu et al., 2016; Chen et al., 2021). This phenological changes in leaf demography is the primary cause of GPP seasonality in TEFs (Saleska et al., 2003; Sayer et al., 2011; Leff et al., 2012) and thus largely regulates their seasonal carbon sinks (Beer et al., 2010; Aragao et al., 2014;

Saatchi et al., 2011).

A key plant trait linking canopy phenology with GPP seasonality was shown to be leaf age (Wu et al., 2017; Xu et al., 2017). At leaf scale, the newly-flushed young leaves and maturing leaves show higher maximum carboxylation rates ($V_{c,max}$) than the old leaves being replaced (de Weirdt et al., 2012; Chen et al., 2020). Such age-dependent variations in $V_{c,max}$ is associated with changes in leaf nutritional contents (nitrogen, phosphorus and potassium etc.) and stomatal conductance over time (Menezes et al., 2021). Xu et al. (2017) and Menezes et al. (2021) monitored in situ leaf age and leaf demography combined with leaf-level $V_{c,max}$ in Amazonian TEFs and found that $V_{c,max}$ of newly-flushed leaves increases rapidly with leaf longevity, peaks at approximately 2-month old and then declines gradually as leaf grows older (leaf age > 2 months). At canopy scale, it is hypothesized that leaf demography and seasonal differences in leaf age compositions of tree canopies control the GPP seasonality in TEFs (Wu et al., 2016; Albert et al., 2018). It has been confirmed that similar mechanism occurs in the ground-based LiDAR observation of upper canopy LAI (more young and mature leaves) increasing during the dry season, whereas lower canopy LAI (more old leaves) decreasing (Smith et al., 2019). Wu et al. (2016) classified canopy leaves of Amazonian TEFs into three leaf age cohorts (young leaves: 1 – 2 months, mature: 3 – 5 months and old: ≥ 6 months) and found that LAI (leaf area index) of young and mature leaves increases and consequently promotes canopy photosynthesis during the dry seasons. Based on above age-dependent $V_{c,max}$ at leaf scale (Xu et al., 2017) and LAI seasonality of different leaf age cohorts at canopy scale (Wu et al., 2016), Chen et al. (2020; 2021) developed a climate-triggered leaf litterfall and flushing model and successfully represented the seasonality of canopy leaf demography and GPP at four Amazonian TEF sites. These studies suggest that leaf age-dependent LAI seasonality is one of the vital biotic factors in influencing the GPP seasonality in TEFs (Wu et al., 2016; Chen et al., 2020).

Although the leaf age-dependent LAI seasonality can be well documented at site level using phenology cameras (Wu et al., 2016), it is still rarely studied and remains unclear at the continental scale. The key causation is that leaf flushing and litterfall of TEFs in different climatic regions experience different seasonal constraints of water and light availability during recurrent dry and wet seasons (Brando et al., 2010; Chen et al., 2020; Davidson et al., 2012; Xiao et al., 2005). Thus, the seasonal patterns of LAI in different leaf age cohorts became very complex at the continental scale (Chen et al., 2020; Xu et al., 2015). Satellite-based remote sensing (Saatchi et al., 2011, Guan et al., 2015) and land surface model (LSM) technologies (de Weirdt et al., 2012; Chen et al., 2020; Chen et al., 2021) are two commonly used approaches for detecting the spatial heterogeneity of plant phenology at a large scale. However, for satellite-based studies, most optical signals are saturated in TEFs due to the dense covered canopies and thus fail to capture the seasonality of total LAI in TEFs, much less decompose the LAI into different leaf age cohorts. These limitations prevented satellite-based studies from accurately representing the age-dependent LAI seasonality. Moreover, most ESM models also show poor performances in simulating the LAI seasonality in different leaf age cohorts (de Weirdt et al., 2012; Chen et al., 2020). This is because that the underling mechanisms linking seasonal water and light availability with leaf flushing and litterfall seasonality are currently highly debated and remain elusive at regional scale (Leff et al., 2012; Saleska et al., 2003; Sayer et al., 2011).

This vague notion imposes a challenge for accurately modeling continental-scale GPP seasonality in most LSMs (Restrepo-Coupe et al., 2017; Chen et al., 2021).

*To fill the research gap, this study aims to produce a grid dataset of leaf age-dependent LAI seasonality product (Lad-LAI) at the continental scale over the TEF biomes from 2001 to 2018. For this purpose, we simplified that canopy GPP was composed of three parts that are produced from young, mature and old leaves, respectively; and based on this assumption, GPP was expressed as a function of the sum of the product of each LAI cohort (i.e., young, mature and old leaves, denoted as LAI_{young}, LAI_{mature}, and LAI_{old}, respectively) and corresponding net CO_2 assimilation rate (An, denoted as An_{young}, An_{mature}, and An_{old} for young, mature and old leaves, respectively) (**Equation 1**). Then, we proposed a novel neighbor-based approach to derive the values of three LAI cohorts. It is hypothesized that forests in adjacent four cells in the grid map exhibit consistent magnitude and seasonality of GPP, LAI_{young}, LAI_{mature}, and LAI_{old}. By applying **Equation 1** to each of the four selected cells, we combined the four equations to derive the three LAI cohorts using a linear least-squares with constrained method. An is calculated using the Farquhar-von Caemmerer-Berry (FvCB) leaf photochemistry model (Farquhar et al., 1980); and GPP is linearly derived from an arguably better proxy—TROPOMI (the TROPOspheric Monitoring Instrument) Solar-Induced Fluorescence (SIF) calibrated by eddy covariance GPP data (**See Methods for details**). This grid dataset of three LAI cohorts provides new insights into tropical and subtropical phenology with more details of sub-canopy level of leaf seasonality in different leaf age cohorts and will be helpful for developing accurate tropical phenology model in ESMs."*

Comment 5: It would be better to add a Study area and data used session to introduce some relevant information and Figure 1.

Response: *We agree with the reviewer that a "2. Study area and material" section is needed, to introduce some relevant information and Figure 1. The text was added in the "Study area and material" as follows:*

*"**2. Study area and material***

2.1 Tropical and subtropical evergreen broadleaved forest biomes

*In this study, we focused on pan tropical and subtropical evergreen broadleaf forests (TEFs). The pixels that belong to TEFs according to the International Geosphere-Biosphere Program (IGBP) classification were extracted as the study area based on the 0.05° spatial resolution MODIS land cover map (**Figure 1**) (MCD12C1, Sulla-Menashe et al., 2018). The study area contains three regions: South American (30°S–18°N; 40°W–90°W), the world's largest and most biodiverse tropical rain forest, Congo (10°S–10°N; 10°E−30°E), the western part of the Africa TEF region, and Tropical Asia (20°S–30°N; 70°E−150°E), covering the Indo-China Peninsula, the majority of the Malay Archipelago and the northern Australia.*

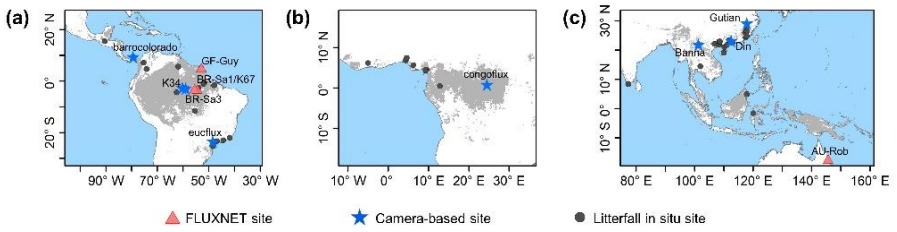

Figure 1. *Study areas over tropical and sub-tropical for evergreen broadleaves forests. Red triangles: four sites of EC-observed GPP seasonality. Blue pentangles: camera-based observation sites of three LAI cohort seasonality. Black circles: observation sites of litterfall seasonality.*

2.2 Input datasets for calculating GPP and An parameters

The TROPOMI (the TROPOspheric Monitoring Instrument) Solar-Induced Fluorescence (SIF) data are used to derive the continent-scale GPP (denoted as RTSIF-derived GPP) according to the SIF-GPP relationship established by Chen et al. (2022). The air temperature data from ERA5-land (Zhao, Gao et al., 2020), vapor pressure deficits (VPD) data from ERA-Interim (Yuan et al., 2019) and downward shortwave solar radiation (SW) from Breathing Earth System Simulator (BESS) (Ryu et al., 2018) were used to calculate K_C, K_O, Γ^*, R_{dark} and $V_{c,max}$ and thus to calculate An according to equations in ***Table S4-part1*** *and* ***Table S4-part4****. The calculation processes were illustrated in* ***Figure 2****. All datasets were aggregated at the same spatial (0.125°) and temporal resolutions (month).*

2.3 Datasets for validating leaf age-dependent LAI seasonality

Ground-based seasonal LAI cohorts and litterfall data. Top-of-canopy imageries observed by phenology cameras were used to decompose the in situ seasonal LAI_{young}, LAI_{mature}, and LAI_{old} data. In total, imageries from eight observation sites across the TEFs are used to validate the simulating results (blue pentangles in ***Fig. 1****,* ***Table S1****). Additionally, the seasonal litterfall data from 53 in situ sites (black circles in* ***Fig. 1****) spanning the TEFs are collected from globally published articles to compare with the phase of LAI_{old} seasonality (see* ***Methods*** *for details). The multiyear monthly litterfall data were averaged to the monthly mean to compare with the simulated seasonality of LAI_{old}. Four eddy covariance flux tower sites (red triangles in* ***Fig. 1****) provide in-situ GPP data to evaluate the seasonality of RTSIF-derived GPP.*

Satellite-based seasonal MODIS EVI data. To evaluate the LAI seasonality of photosynthesis-effective leaves, i.e. young and mature leaves, this study used satellite-based MODIS Enhanced Vegetation Index (EVI) from independent sensors (Huete et al., 2002; Lopes et al., 2016; Wu et al., 2018) as a remotely sensed proxies alternatives of effective leaf area changes and new leaf flush, i.e., $LAI_{young+mature}$ (Wu et al., 2016; Xu et al., 2015). To prove the robustness of the products over a large spatial coverage, the seasonal LAI cohorts of young and mature leaves are evaluated against the enhanced vegetation index (EVI) product, which is considered as a proxy for leaf area changes of photosynthetic effective leaves (Xu et al., 2015; Wu et al., 2016).”

Comment 6: Authors used a constant value (LAI = 7) of total LAI in tropical and subtropical EBFs., but the valid range of LAI is generally 0 to 10. Thus, I expect to see more evidence for selecting 7 or a sensitivity analysis of threshold can also be implemented.

Response*: Thanks for your valuable comment regarding the selection of LAI constant in our manuscript. We have thoroughly collected relative studies to determine the appropriate LAI for tropical and subtropical EBFs. Results were shown in Figure R1, R2 and Table R1. Results showed that there are slightly spatial and seasonal variations in totally LAI (around 6.0) across the pantropical forests. Thus, we have revised the LAI constant value to 6 in the revised manuscript and updated Lad-LAI products accordingly.*

Table R1. *Information of total LAI mean values from the references.*

NO.	LAI mean	Sites	Methods	Ref.
1	6.0	ORCHIDEE TrBE module	Module	de Weirdt et al., 2012
2	5.88	K34	observation	Wu et al., 2016
3	5.45	Tapajo´s National Forest	observation	Asner et al., 2003
4	6.04	Barro Colorado Island	observation	Wirth et al., 2001
5	6.0	Costa Rican Forest	observation	Clark et al., 2008;
6	5.89	K67	observation	Wu et al., 2016
7	5.9	Tapajo´s National Forest	observation	Brando et al., 2008
8	5.7	K67	observation	Smith et al., 2019
9	5.34	Congo	observation	de Wasseige et al., 2003
10	5.93	Xishuangbanna	observation	Li et al., 2010
11	5.67	Dinhushan	observation	Zhao, Chen et al., 2020

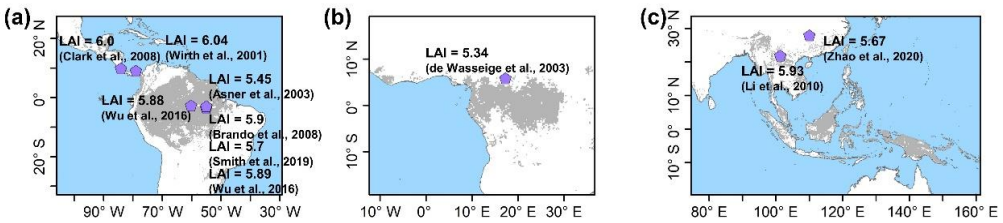

Figure R1. *The measured LAI sites distribution map.*

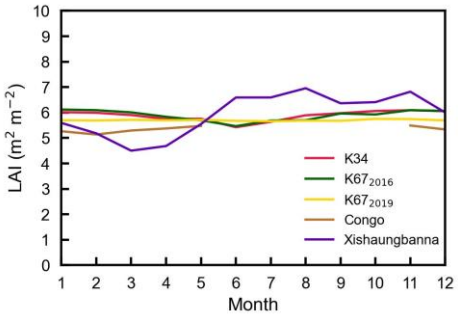

Figure R2. *The seasonality of observed total LAI values from other studies.*

Comment 7: The format of Equation (1) should be: GPP = $LAIyoung \times Anyoung + LAImature \times Anmature + LAIold \times Anold$.

Response: *Thanks for the correction. We have revised Equation (1) as GPP =* $LAIy_{oung} \times An_{young} + LAI_{mature} \times An_{mature} + LAI_{old} \times An_{old}$. *according to your suggestion.*

Comment 8: It is weird why all R values are 0.99 in Fig.3?

Response: *It is a typo. We have revised the R values of this figure and moved it to Supplementary Figures as Figure S1 in the revised manuscript.*

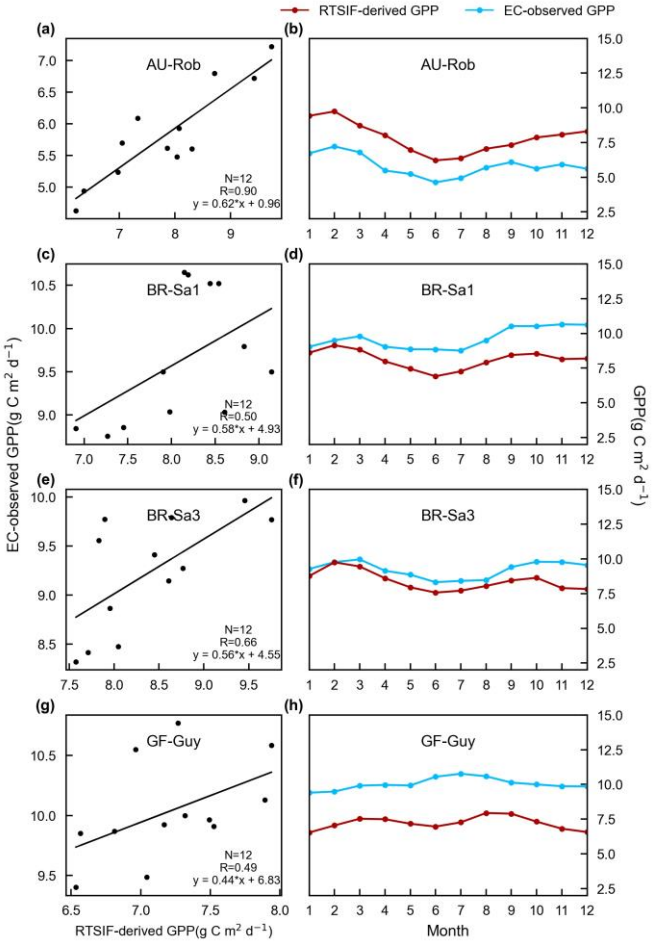

Figure S1. *Comparisons between monthly RTSIF-derived GPP (red) and EC-observed GPP (blue). (a-b) Au-Rob, (c-d) BR-Sa1, (e-f) BR-Sa3, and (g-h) GF-Guy.*

Comment 9: Fig.3 is not supposed to place at Method part, can move it into results or supplementary materials; and Fig.4 is not a contribution of this work, can move it into supplementary materials.

Response: *Thanks. We have moved Figure 3 and Figure 4 to the Supplementary Figures Figure S1 and Figure S2, respectively, as suggested by the reviewer.*

Comment 10: Lines 351-355, can provide some scatterplots between Lad-LAI products and sites observations, rather than providing quantified accuracy metrics only.

Response: *It is a nice suggestion. We have added scatterplots between Lad-LAI products and sites observations in Figures 3-5 right panel. The scatterplots are shown as follows.*

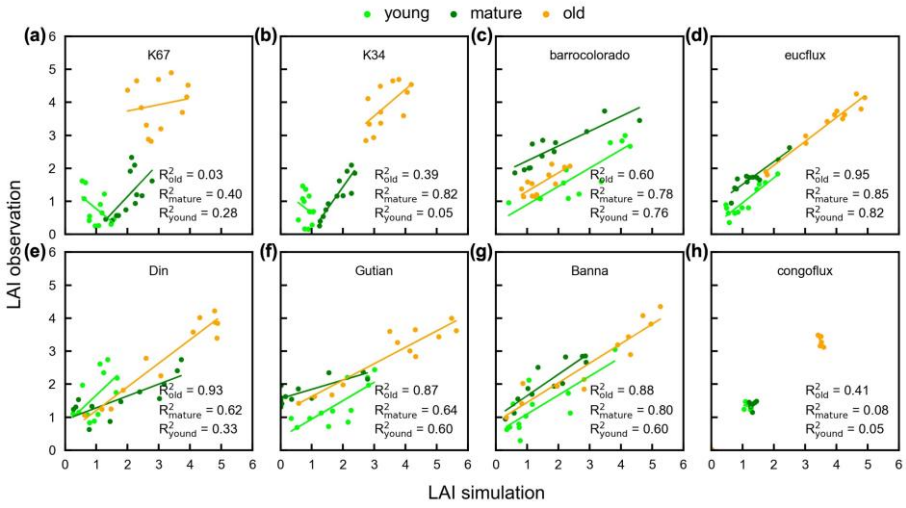

Figure R3. *The scatterplots of simulated LAIs against observed LAIs at 8 camera-based observation sites across study area.*

Reference:

Albert, L. P., Wu, J., Prohaska, N., de Camargo, P. B., Huxman, T. E., Tribuzy, E. S., Ivanov, V. Y., Oliveira, R. S., Garcia, S., Smith, M. N., Oliveira Junior, R. C., Restrepo-Coupe, N., da Silva, R., Stark, S. C., Martins, G. A., Penha, D. V., and Saleska, S. R.: Age-dependent leaf physiology and consequences for crown-scale carbon uptake during the dry season in an Amazon evergreen forest, New Phytol, 219, 870-884, 10.1111/nph.15056, 2018.

Aragao, L. E., Poulter, B., Barlow, J. B., Anderson, L. O., Malhi, Y., Saatchi, S., Phillips, O. L., and Gloor, E.: Environmental change and the carbon balance of Amazonian forests, Biol Rev Camb Philos Soc, 89, 913-931, 10.1111/brv.12088, 2014.

Asner, G.P., Scurlock, J.M.O. and A. Hicke, J.: Global synthesis of leaf area index observations: implications for ecological and remote sensing studies. Global Ecology and Biogeography, 12: 191-205. https://doi.org/10.1046/j.1466-822X.2003.00026.x .2003.

Beer, C., Reichstein, M., Tomelleri, E., Ciais, P., Jung, M., Carvalhais, N., Rodenbeck, C., Arain, M. A., Baldocchi, D., Bonan, G. B., Bondeau, A., Cescatti, A., Lasslop,

G., Lindroth, A., Lomas, M., Luyssaert, S., Margolis, H., Oleson, K. W., Roupsard, O., Veenendaal, E., Viovy, N., Williams, C., Woodward, F. I., and Papale, D.: Terrestrial gross carbon dioxide uptake: global distribution and covariation with climate, Science, 329, 834-838, 10.1126/science.1184984, 2010.

Brando, P. M., Nepstad, D. C., Davidson, E. A., Trumbore, S. E., Ray, D. and Camargo, P.: Drought effects on litterfall, wood production and belowground carbon cycling in an Amazon forest: results of a throughfall reduction experiment. Philosophical Transactions of the Royal Society B: Biological Sciences, 363(1498), 1839-1848. doi: 10.1098/rstb.2007.0031. 2008.

Brando, P. M., Goetz, S. J., Baccini, A., Nepstad, D. C., Beck, P. S., and Christman, M. C.: Seasonal and interannual variability of climate and vegetation indices across the Amazon. Proceedings of the National Academy of Sciences, 200908741. 2010.

Chen, X., Huang, Y., Nie, C., Zhang, S., Wang, G., Chen, S., and Chen, Z.: A long-term reconstructed TROPOMI solar-induced fluorescence dataset using machine learning algorithms, Sci Data, 9, 427, 10.1038/s41597-022-01520-1, 2022.

Chen, X., Maignan, F., Viovy, N., Bastos, A., Goll, D., Wu, J., Liu, L., Yue, C., Peng, S., Yuan, W., Conceição, A. C., O'Sullivan, M., and Ciais, P.: Novel Representation of Leaf Phenology Improves Simulation of Amazonian Evergreen Forest Photosynthesis in a Land Surface Model, Journal of Advances in Modeling Earth Systems, 12, 10.1029/2018ms001565, 2020.

Chen, X., Ciais, P., Maignan, F., Zhang, Y., Bastos, A., Liu, L., Bacour, C., Fan, L., Gentine, P., Goll, D., Green, J., Kim, H., Li, L., Liu, Y., Peng, S., Tang, H., Viovy, N., Wigneron, J. P., Wu, J., Yuan, W., and Zhang, H.: Vapor Pressure Deficit and Sunlight Explain Seasonality of Leaf Phenology and Photosynthesis Across Amazonian Evergreen Broadleaved Forest, Global Biogeochemical Cycles, 35, 10.1029/2020gb006893, 2021.

Clark, D.B., Olivas, P.C., Oberbauer, S.F., Clark, D.A. and Ryan, M.G.: First direct landscape-scale measurement of tropical rain forest Leaf Area Index, a key driver of global primary productivity. Ecology Letters, 11: 163-172. https://doi.org/10.1111/j.1461-0248.2007.01134.x 2008.

Davidson, E. A., de Araújo, A. C., Balch, J. K., Brown, I. F., Bustamante, M. M., et al.: The Amazon basin in transition. Nature, 481(7381), 321–328. https://doi.org/10.1038/nature10717. *2012.*

de Wasseige, C., Bastin, D. and Defourny, P.: Seasonal variation of tropical forest LAI based on field measurements in Central African Republic. Agricultural and Forest Meteorology, 119(3-4), 181-194. doi: 10.1016/S0168-1923(03)00138-2. 2003.

de Weirdt, M., Verbeeck, H., Maignan, F., Peylin, P., Poulter, B., Bonal, D., Ciais, P., and Steppe, K.: Seasonal leaf dynamics for tropical evergreen forests in a process-based global ecosystem model, Geoscientific Model Development, 5, 1091-1108, 10.5194/gmd-5-1091-2012, 2012.

Farquhar, G. D., von Caemmerer, S., and Berry, J. A.: A biochemical model of photosynthetic CO2 assimilation in leaves of C 3 species, Planta, 149, 78-90, 10.1007/BF00386231, 1980.

Guan, K., Pan, M., Li, H., Wolf, A., Wu, J., Medvigy, D., Caylor, K. K., Sheffield, J.,

Wood, E. F., Malhi, Y., Liang, M., Kimball, J. S., Saleska, Scott R., Berry, J., Joiner, J., and Lyapustin, A. I.: Photosynthetic seasonality of global tropical forests constrained by hydroclimate, Nature Geoscience, 8, 284-289, 10.1038/ngeo2382, 2015.

Huete, A., Didan, K., Miura, T., Rodriguez, E. P., Gao, X., and Ferreira, L. G.: Overview of the radiometric and biophysical performance of the MODIS vegetation indices, Remote Sensing of Environment, 83, 195-213, 10.1016/s0034-4257(02)00096-2, 2002.

Leff, J. W., Wieder, W. R., Taylor, P. G., Townsend, A. R., Nemergut, D. R., Grandy, A. S., and Cleveland, C. C.: Experimental litterfall manipulation drives large and rapid changes in soil carbon cycling in a wet tropical forest. Global Change Biology, 18(9), 2969–2979. https://doi.org/10.1111/j.1365-2486.2012.02749.x. 2012.

Li, Z., Zhang, Y., Wang, S., Yuan, G., Yang, Y. and Cao, M.: Evapotranspiration of a tropical rain forest in Xishuangbanna, southwest China. Hydrol. Process., 24: 2405-2416. https://doi.org/10.1002/hyp.7643. *2010.*

Lopes, A. P., Nelson, B. W., Wu, J., Graça, P. M. L. d. A., Tavares, J. V., Prohaska, N., Martins, G. A., and Saleska, S. R.: Leaf flush drives dry season green-up of the Central Amazon, Remote Sensing of Environment, 182, 90-98, 10.1016/j.rse.2016.05.009, 2016.

Menezes, J., Garcia, S., Grandis, A., Nascimento, H., Domingues, T. F., Guedes, A. V., Aleixo, I., Camargo, P., Campos, J., Damasceno, A., Dias-Silva, R., Fleischer, K., Kruijt, B., Cordeiro, A. L., Martins, N. P., Meir, P., Norby, R. J., Pereira, I., Portela, B., Rammig, A., Ribeiro, A. G., Lapola, D. M., and Quesada, C. A.: Changes in leaf functional traits with leaf age: when do leaves decrease their photosynthetic capacity in Amazonian trees? Tree Physiology, 42(5), 922-938, https://doi.org/10.1093/treephys/tpab042, 2021.

Pan, Y., Birdsey, R. A., Fang, J., Houghton, R., Kauppi, P. E., Kurz, W. A., et al.: A large and persistent carbon sink in the world's forests. Science, 333(6045), 988–993. https://doi.org/10.1126/science.1201609, 2011.

Restrepo-Coupe, N., Levine, N. M., Christoffersen, B. O., Albert, L. P., Wu, J., Costa, M. H., Galbraith, D., Imbuzeiro, H., Martins, G., da Araujo, A. C., Malhi, Y. S., Zeng, X., Moorcroft, P., and Saleska, S. R.: Do dynamic global vegetation models capture the seasonality of carbon fluxes in the Amazon basin? A data-model intercomparison, Glob Chang Biol, 23, 191-208, 10.1111/gcb.13442, 2017.

Ryu, Y., Baldocchi, D. D., Kobayashi, H., van Ingen, C., Li, J., Black, T. A., Beringer, J., van Gorsel, E., Knohl, A., Law, B. E., and Roupsard, O.: Integration of MODIS land and atmosphere products with a coupled-process model to estimate gross primary productivity and evapotranspiration from 1 km to global scales, Global Biogeochemical Cycles, 25, n/a-n/a, 10.1029/2011gb004053, 2011.

Saatchi, S. S., Harris, N. L., Brown, S., Lefsky, M., Mitchard, E. T., Salas, W., Zutta, B. R., Buermann, W., Lewis, S. L., Hagen, S., Petrova, S., White, L., Silman, M., and Morel, A.: Benchmark map of forest carbon stocks in tropical regions across three continents, Proc Natl Acad Sci U S A, 108, 9899-9904, 10.1073/pnas.1019576108,

2011.

Saleska, S. R., Miller, S. D., Matross, D. M., Goulden, M. L., Wofsy, S. C., da Rocha, H. R., de Camargo, P. B., Crill, P., Daube, B. C., de Freitas, H. C., Hutyra, L., Keller, M., Kirchhoff, V., Menton, M., Munger, J. W., Pyle, E. H., Rice, A. H., and Silva, H.: Carbon in Amazon forests: unexpected seasonal fluxes and disturbance-induced losses, Science, 302, 1554-1557, 10.1126/science.1091165, 2003.

Sayer, E. J., Heard, M. S., Grant, H. K., Marthews, T. R., and Tanner, E. V. J.: Soil carbon release enhanced by increased tropical forest litterfall. Nature Climate Change, 1(6), 304–307. https://doi.org/10.1038/nclimate1190. 2011.

Smith, M. N., Stark, S. C., Taylor, T. C., Ferreira, M. L., de Oliveira, E., Restrepo-Coupe, N., Chen, S., Woodcock, T., dos Santos, D. B., Alves, L. F., Figueira, M., de Camargo, P. B., de Oliveira, R. C., Aragão, L. E. O. C., Falk, D. A., McMahon, S. M., Huxman, T. E. and Saleska, S. R.: Seasonal and drought-related changes in leaf area profiles depend on height and light environment in an Amazon forest. New Phytol, 222: 1284-1297. https://doi.org/10.1111/nph.15726. 2019.

Sulla-Menashe, D., Woodcock, C. E., and Friedl, M. A.: Canadian boreal forest greening and browning trends: An analysis of biogeographic patterns and the relative roles of disturbance versus climate drivers. Environmental Research Letters, 13(1), 014007, 2018.

Wirth, R., Weber, B., and Ryel, R. J.: Spatial and temporal variability of canopy structure in a tropical moist forest. Acta Oecologica, 22(5-6). 2001.

Wu, J., Albert, L. P., Lopes, A. P., Restrepo-Coupe, N., Hayek, M., Wiedemann, K. T., Guan, K., Stark, S. C., Christoffersen, B., Prohaska, N., Tavares, J. V., Marostica, S., Kobayashi, H., Ferreira, M. L., Campos, K. S., da Silva, R., Brando, P. M., Dye, D. G., Huxman, T. E., Huete, A. R., Nelson, B. W., and Saleska, S. R.: Leaf development and demography explain photosynthetic seasonality in Amazon evergreen forests, Science, 351, 972-976, 10.1126/science.aad5068, 2016.

Wu, J., Guan, K., Hayek, M., Restrepo-Coupe, N., Wiedemann, K. T., Xu, X., et al.: Partitioning controls on Amazon forest photosynthesis between environmental and biotic factors at hourly to interannual timescales. Global Change Biology, 23(3), 1240–1257. https://doi.org/10.1111/gcb.13509. 2017.

Wu, J., Kobayashi, H., Stark, S. C., Meng, R., Guan, K., Tran, N. N., Gao, S., Yang, W., Restrepo-Coupe, N., Miura, T., Oliviera, R. C., Rogers, A., Dye, D. G., Nelson, B. W., Serbin, S. P., Huete, A. R., and Saleska, S. R.: Biological processes dominate seasonality of remotely sensed canopy greenness in an Amazon evergreen forest, New Phytol, 217, 1507-1520, 10.1111/nph.14939, 2018.

Xiao, X., Zhang, Q., Saleska, S., Hutyra, L., De Camargo, P., Wofsy, S., Frolking, S., Boles, S., Keller, M., and Moore, B.: Satellite-based modeling of gross primary production in a seasonally moist tropical evergreen forest, Remote Sensing of Environment, 94, 105-122, 10.1016/j.rse.2004.08.015, 2005.

Xu, L., Saatchi, S. S., Yang, Y., Myneni, R. B., Frankenberg, C., Chowdhury, D., and Bi, J.: Satellite observation of tropical forest seasonality: spatial patterns of carbon exchange in Amazonia, Environmental Research Letters, 10, 10.1088/1748-9326/10/8/084005, 2015.

Xu, X., Medvigy, D., Joseph Wright, S., Kitajima, K., Wu, J., Albert, L. P., Martins, G. A., Saleska, S. R., and Pacala, S. W.: Variations of leaf longevity in tropical moist forests predicted by a trait-driven carbon optimality model, Ecol Lett, 20, 1097-1106, 10.1111/ele.12804, 2017.

Yuan, W., Zheng, Y., Piao, S., Ciais, P., Lombardozzi, D., Wang, Y., Ryu, Y., Chen, G., Dong, W., Hu, Z., Jain, A. K., Jiang, C., Kato, E., Li, S., Lienert, S., Liu, S., Nabel, J., Qin, Z., Quine, T., Sitch, S., Smith, W. K., Wang, F., Wu, C., Xiao, Z., and Yang, S.: Increased atmospheric vapor pressure deficit reduces global vegetation growth, Sci Adv, 5, eaax1396, 10.1126/sciadv.aax1396, 2019.

Zhao, P., Gao, L., Wei, J., Ma, M., Deng, H., Gao, J., and Chen, X.: Evaluation of ERA-Interim Air Temperature Data over the Qilian Mountains of China. Advances in Meteorology, 7353482. https://doi.org/10.1155/2020/7353482, 2020.

Zhao, Y., Chen, X., Smallman, T. L., Flack-Prain, S., Milodowski, D. T., and Williams, M.: Characterizing the Error and Bias of Remotely Sensed LAI Products: An Example for Tropical and Subtropical Evergreen Forests in South China. Remote Sensing. 12(19):3122. https://doi.org/10.3390/rs12193122. 2020.